SEMARAK ILMU PUBLISHING

Journal of Advanced Research in Fluid Mechanics and Thermal Sciences

Journal homepage:
https://semarakilmu.com.my/journals/index.php/fluid_mechanics_thermal_sciences/index
ISSN: 2289-7879

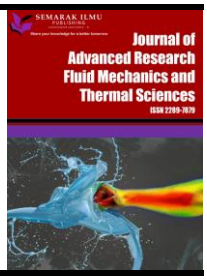

Performance Analysis of a Crossflow Vortex Turbine for a Gravitational Water Vortex Power Plant

Abel Alfeuz[1], Fadzlita Tamiri[1], Farm Yan Yan[1], Wan Khairul Muzammil[1], Melvin Gan Jet Hong[1], Dayang Salyani Abang Mahmod[2], Nuramalina Bohari[3], Mohd Azlan Ismail[1,*]

[1] Faculty of Engineering, Universiti Malaysia Sabah, Kota Kinabalu, Sabah, Malaysia
[2] Department of Chemical Engineering and Energy Sustainability, Universiti Malaysia Sarawak, Kuching, Sarawak, Malaysia
[3] School of Engineering & Technology, University of Technology Sarawak, Sibu, Sarawak, Malaysia

ARTICLE INFO

Article history:
Received 4 October 2023
Received in revised form 24 March 2024
Accepted 3 April 2024
Available online 30 April 2024

Keywords:
Micro hydropower; gravitational water vortex power plant; water vortex; crossflow turbine; velocity profile; power; efficiency

ABSTRACT

The micro hydro system is the most favorable renewable energy source to supply electricity for rural areas. The Gravitational Water Vortex Power Plant (GWVPP) is one of the micro hydro systems that is suitable for very low-head hydropower sites. GWVPP consists of three major parts: electromechanical components, civil structures, and electric distribution. The micro hydro turbine in GWVPP is called a vortex hydro turbine and is used to convert induced vortex flow to mechanical energy coupled with a generator to produce electricity. This paper investigates crossflow vortex turbine performance using Computational Fluid Dynamics (CFD) software and experimental work. The CFD results provide qualitative and quantitative comprising velocity distribution, water vortex profile, and water vortex height. The optimum hydraulic performance in the water vortex was observed and determined for different turbine positions. The vortex crossflow turbine was placed 0.05 m from the bottom surface of the basin at the highest vortex tangential velocity. A 0.05 m turbine position was chosen for the turbine installations as it creates a high-velocity profile. The comparative performance was conducted on the vortex crossflow blade with different inlet blade angle designs at a range of 40^0 – 70^0. The experimental analysis was conducted at rotational speeds of 30 rpm – 70 rpm to determine its efficiency performance. The optimum design for the crossflow blade was at 50^0 with an operational speed of 50 rpm, which exhibited torque and power output at 0.27±0.02 m and 1.49±0.08 m respectively with an efficiency recorded at 18.98%.

1. Introduction

Hydropower contributes the highest world's renewable energy resources, accounting for more than 16% of net electricity output [1]. Despite the rise in the popularity of wind and solar energy in recent years, hydropower leads as a power generation with 55% of the total power generation capacity from renewable resources [2].

* *Corresponding author.*
E-mail address: lanz_mr@ums.edu.my

https://doi.org/10.37934/arfmts.116.2.1326

Hydropower produces energy by harnessing the kinetic energy of the flowing water. The movement of the turbines converts the kinetic energy of water into mechanical energy, which is then transformed into electrical energy using the electric generator. This process allows hydropower to generate clean energy from the natural energy of flowing water. According to Ullah *et al.,* [3], hydropower can be the primary source of future energy production as it can offer clean and renewable electricity.

The Gravitational Water Vortex Power Plant (GWVPP) is one of the prominent types of hydropower that has attracted attention in recent years [1,2]. GWVPP has recently become an alternative option for electricity generation and can operate at very low head sites ranging from 0.7 m to 2.0m [4]. GWVVP operates by using induced vortex flow producing tangential inlet velocity that creates a rotating flow due to the conservation of momentum. The water exits at the basin opening producing an air core in the middle of the vortex flow [3].

Other than that, GWVPP is a considerably low investment cost due to its versatility; suitable for retrofit to existing infrastructure [5]. In 2006, the investment cost for 10 kW of GWVPP was reported at 60,000€, relatively lower compared to conventional types of hydro turbines [6]. One of the main reasons for the lower cost of GWVPP is does not require a big reservoir or installation footprint [2]. In addition, GWVPP is designed for very low-head rivers, located at relatively flat hydropower sites, thus further reducing the overall installation cost.

The GWVPP consists of two parts: 1) the civil structure consists of a water inlet, open channel, and basin 2) the electromechanical components consist of a turbine, shaft, and electric generator [3]. The civil structure of the GWVPP collects and diverts water from the river and channels the water to the GWVVP basin. Induced vortex flow intensity and performance are subject to the geometric size and shape of the civil structure. Potential energy from height difference between inlet water and outlet opening of the basin induced vortex flow, conversion to kinetic energy. Electromechanical components consist of hydro turbines that convert kinetic energy to mechanical energy. The turbine performance is strongly dependent on the vortex strength with a stable vortex profile. In this regard, it is significant to determine the pattern of a stable vortex profile for turbine optimization. By coupling the turbine blade with an electric generator, the mechanical energy is then converted into electrical energy.

There is intensive research interest in improving turbine blade efficiency through blade geometry modification by considering its rotational effect on the swirling flow of the vortex. This is especially important for high-efficiency operations at optimum runner shape that relies on the appropriate design of the turbine blade profiles [4]. Dhakal *et al.,* [5] performed a comparative investigation on the three different blade profiles using CFD. The comparative data are based on the turbine efficiency performance, and it was found that the curved blade profiles yield significance high efficiency at 82% followed by twisted and straight blade profiles which are 63% and 46% respectively.

Then, Kayastha *et al.,* [6] obtained a 35.59% enhancement in turbine efficiency using curved blade profiles with optimum turbine position and Kueh *et al.,* [7] found that the turbine efficiency could be increased by about 22.24% using curved blade profiles based on the constant operating speed. Other than that, Nishi *et al.,* [8] achieved improvement in turbine performance using crossflow blade profiles as they found the hydraulic losses from the interactions between the water and the turbine blade can be minimized, and the power efficiency output could be about 55%. In addition, Aziz *et al.,* [9] conducted an experimental study using a flat turbine in the enclosed gravitational water vortex system and found a maximum mechanical efficiency of 16.06% with the best efficient point at 6.3 L/s of water flow rate. Whilst Del Rio *et al.,* [10] numerically study the torque produced at different rotational speeds and in this case, the H-Darrieus type of turbine was used as the rotor in the water vortex turbine, and they found that the maximum torque was at 50 RPM. Moreover, Aziz *et al.,* [11]

found that the maximum torque of 15.31 N can be produced using 12 runner blades at 90^o blade angle.

Nevertheless, the reports on the effects of the turbine blade angles on the turbine performance are very limited. This work conducted a systematic study on the effects of turbine blade angle for turbine performance analysis using crossflow blade profiles. An in-depth observation was done on the torque, rotational speed, power output, and power efficiency. To the best of our knowledge, the modification of the turbine blade angle using crossflow blade profiles has the opportunity for further discoveries to improve the vortex turbine performance.

2. Theoretical Power of the GWVPP

Power input from hydropower is dependent on the head and flow rate based on the site and determined as

$$P_{in} = \rho g Q h \tag{1}$$

where ρ is the density of the water, g is the gravity constant, Q is the flow rate passing through the turbine from the inlet and h is the head. The performance of GWVPP is derived through its output efficiency and it is like the other conventional turbines. The turbine in GWVPP is often classified as an impulse turbine and the equation is written as

$$P_{out} = \mathrm{T}\omega \tag{2}$$

where T is the shaft's generated torque and ω is the impeller angular velocity. Since the rotation axis of the turbine is selected in the y-direction. The impeller angular velocity can be calculated using the equation

$$\omega = \frac{2\pi N}{60} \tag{3}$$

Where N is the rotational speed of the impeller. Thus, the efficiency of the turbine in GWVPP can be expressed as

$$\eta = \frac{P_{out}}{P_{in}} = \frac{\mathrm{T}\omega}{\rho g Q h} \tag{4}$$

3. The Design of Crossflow Vortex Turbine

The design of the crossflow vortex turbine blade has been carried out using the principle of the velocity triangle. The crossflow vortex turbine uses the same inlet velocity cases in which the water from the inlet channel (V_1) contacts the turbine blade through the basin. Figure 1 shows a crossflow vortex turbine with 18 number of blades. Particularly, the number of blades was based on the Sritram and Suntivarakorn [12] study which found that the 18-blade configuration yielded an optimum efficiency performance. These blades are designed in a curved shape with relative and absolute velocity vectors fixed to both the leading and trailing edge at the blade tip, where: U is the blade velocity, β is the blade angle, α is the absolute angle, V is the absolute velocity, V_r is the radial velocity, V_ω is the whirl velocity and V_f is the flow velocity.

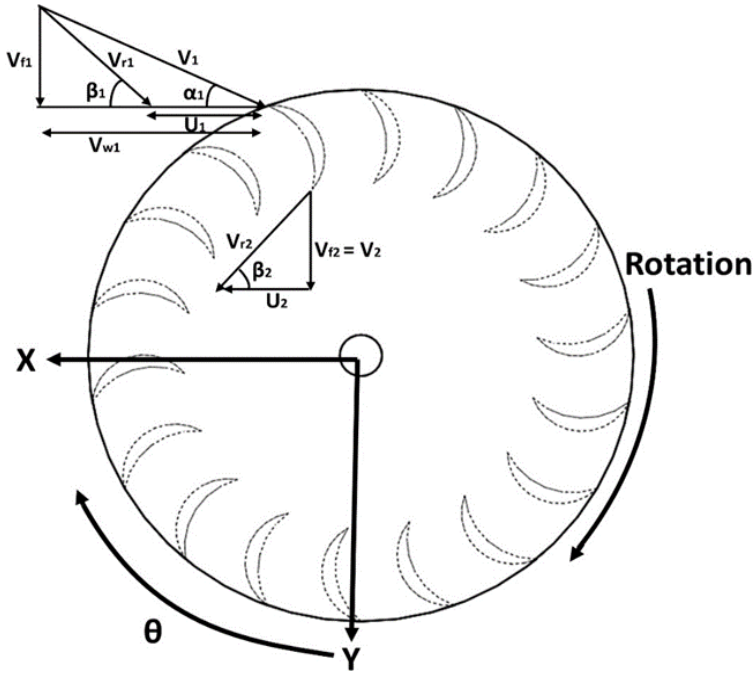

Fig. 1. Velocity triangle for blade profile

4. Dimension and Features of the GWVPP System

In the current study, the configurations of a cylindrical basin of the GWVPP were designed using a standard scroll-type vortex drop shaft with a flat bottom to maintain subcritical approach flow conditions. Figure 2 represents the geometrical parameters of the GWVPP mechanism with the specific dimensions that were implemented using SOLIDWORKS software.

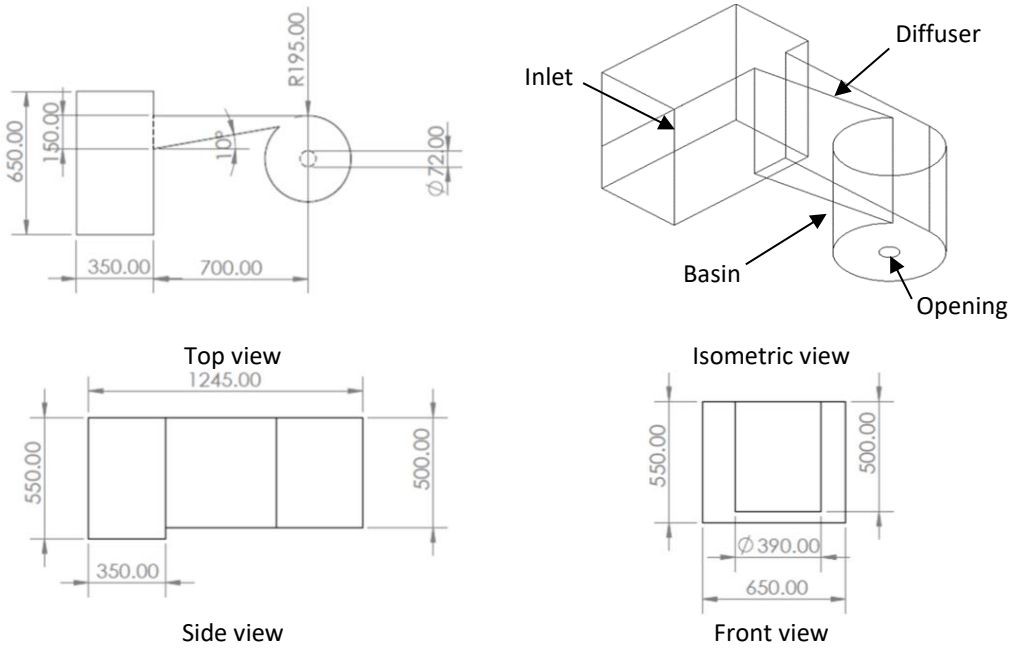

Fig. 2. GWVPP dimensions and features

(a) An **Inlet channel** is a mechanism in the GWVPP that directs the flow of water from the reservoir towards the basin.
(b) A **Diffuser** is a mechanism that allows the water to flow tangentially into a basin.

(c) The **basin** is a circular cylinder that creates a symmetrical vortex flow.
(d) An **opening** is a mechanism at the bottom of the basin that discharges the water flow.

5. Computational Fluid Dynamics (CFD) Simulation

In this section, the qualitative results from the CFD simulation model are presented to determine the performance of an induced vortex flow. The qualitative result of this study is to investigate the dynamic flow in the induced vortex flow. The CFD is a tool to investigate the performance of an induced vortex flow. The results from the simulation model can be used to identify the optimum turbine position in the basin. The water vortex height, vortex strength, and velocity profile will be observed to clarify the performance of induced vortex flow performance. Moreover, the blade profile of the crossflow turbine will be designed based on simulation results.

As shown in Figure 3(a) shows 3D model represents computational domains for the wetted volume consisting of inlet, diffuser, and basin. The CAD model was taken as the computational domain and meshed in ANSYS CFX. The ANSYS CFX is a module of ANSYS software that enables the creation of structured grids for complex geometries.

Figure 3(b) illustrates an unstructured tetrahedral shape in all flow regions. The function of this mesh is to solve complex geometric topologies and to capture the flow physics in the domain. The mesh elements are 0.0012 m and have relatively fine grids for all surfaces. Then, the number of elements for the volute elements and the number of nodes were recorded at 655574 and 122351 respectively.

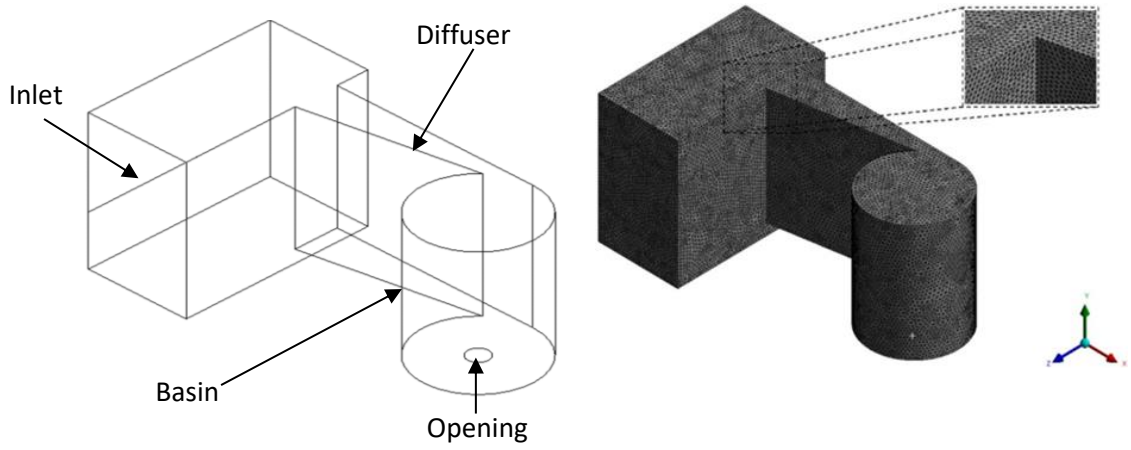

(a) (b)

Fig. 3. (a) CAD Domain, (b) Meshing Topography

Figure 4 represents the boundary condition of the GWVPP. The interfaces of the boundary condition for these domains were set according to their physical flow. The condition includes a steady flow, no-slip condition, and the two fluids (air and water) in the same region. The domain and reference pressure temperature were set to 25 ^{o}C and 0 atm respectively. Then, the buoyancy reference density for the water was 1.2 kg/m^3 and the surface tension coefficient was set to 0.072 N/m. The computational domains were simulated with no-slip conditions at the wall and pressure outlet conditions at the outlet. Other than that, the inlet flow rate of 0.004 m^3/s was set at the inlet channel. For the top surface, the boundary conditions were subjected to atmospheric pressure.

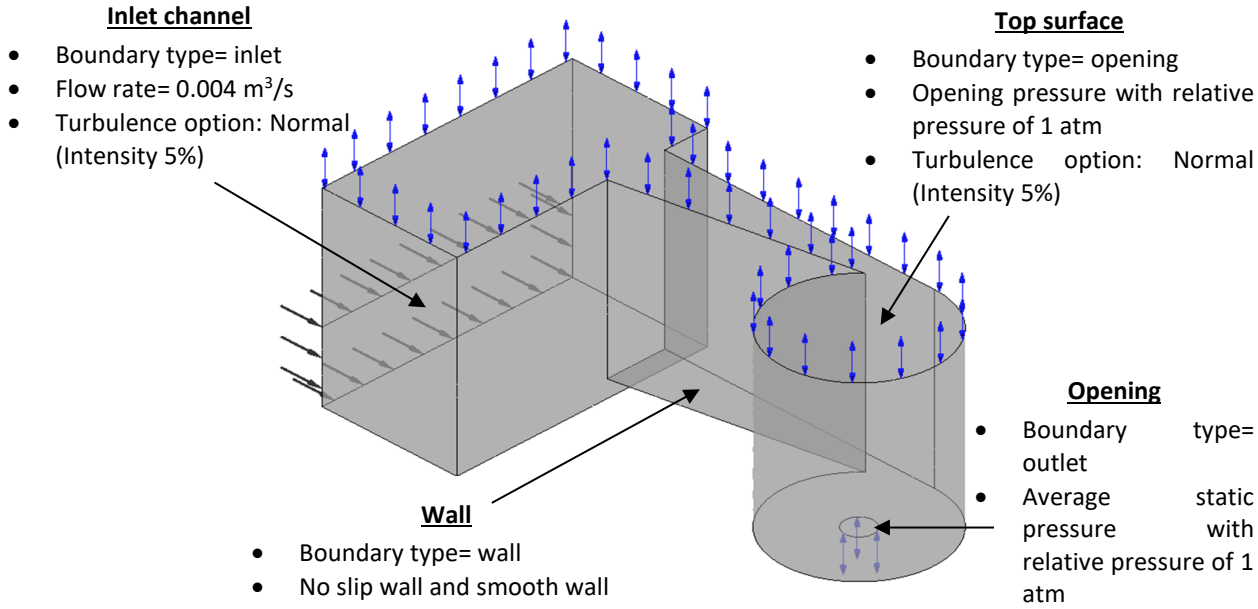

Fig. 4. Boundary conditions and interfaces

In this study, the fluid dynamic problems were presented in non-linear equations governed by the Navier-Stroke equations. They were solved iteratively by numerical methods which lead to convergence criteria. The residuals for each computational domain were plotted at the end of the time step to measure the convergence criteria. To meet the specific convergence criteria, the Residual Root Mean Square (RMS) was set to 0.0001, the domain had imbalances of less than 1% of their value or the values of interest had reached a steady solution.

Figure 5 visualizes the velocity profile at the basin surfaces. The basin surfaces were used as a reference for plane X to determine the velocity profile. In this velocity profile, the intenser color of red and blue indicates the fastest tangential velocity flow of the vortex that was recorded in Figure 5. The tangential velocity increases when the fluid flow reaches the bottom of the water vortex as well as increases the kinetic energy [13]. The region close to the bottom of the water vortex displays the highest hydraulic energy that can produce maximum rotational speed and torque for the turbine to produce optimum electrical power.

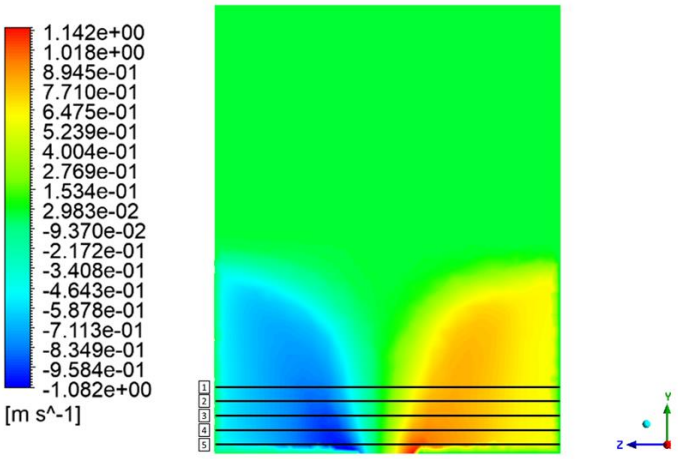

Fig. 5. Velocity Profile

Table 1 depicts the turbine's reference position from the bottom surface of the basin. The reference position was determined by generating the line in the velocity profile as shown in Figure 5. This reference position was used to determine the tangential velocity distribution in the water vortex. Particularly, the reference turbine position was from 0.05-0.25 m from the bottom surface of the water vortex. The highest tangential velocity was 0.741m/s at the position of 0.05 m from the bottom surface of the water vortex. At this 0.05 m, the tangential velocity is recorded at 0.741 m/s and was used as a velocity triangle value to develop the crossflow vortex turbine profile.

Table 1
Turbine's position from the bottom surface

Distance (m)	Turbine position (m)	Tangential velocity (m.s)
Location 1	0.25	0.703
Location 2	0.20	0.711
Location 3	0.15	0.724
Location 4	0.10	0.733
Location 5	0.05	0.741

Figure 6 displays the tangential velocity distribution at different locations in the water vortex. The optimum turbine position was found at 0.05 m (location 5) from the water vortex's bottom surface. It was found that a symmetrical vortex and high tangential velocity were recorded at location 5. An asymmetrical vortex profile can ensure the forces acting on the turbine are balanced which will increase the durability of the turbine. When water flows symmetrically across the turbine, it reduces the lateral forces or imbalances that produce excessive stress on the turbine [14]. Therefore, the turbine is expected to extract stable torque and power when the turbine is positioned close to the bottom of the water vortex.

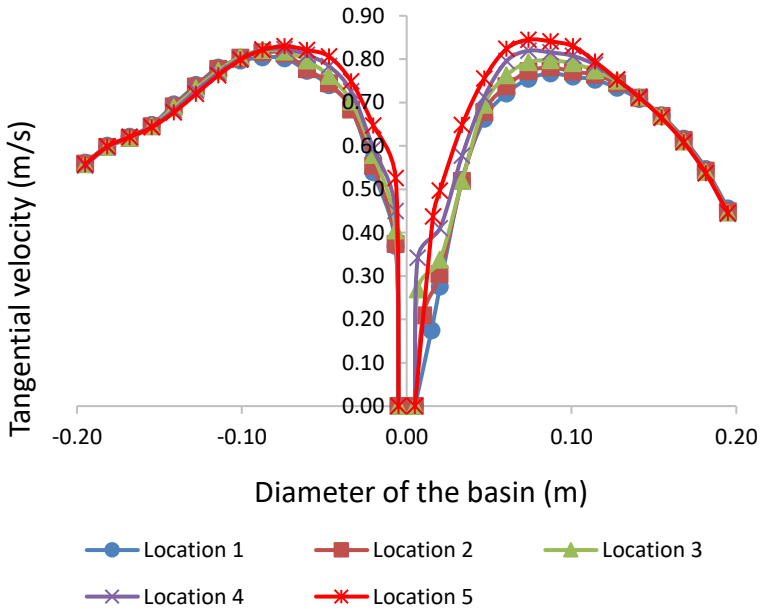

Fig. 6. Tangential velocity distribution

6. Experimental Setup of the GWVPP

A complete experimental setup was built in the laboratory of the Hydraulic Engineering Faculty to determine the performance of a GWVPP by using the crossflow turbine. The setup comprises the centrifugal pump, flow meter, torque sensor, band brake, water tank, runner blade, data logger, basin, water reservoir, and diffuser installed along the inlet channel as shown in Figure 7. The torque sensor was mounted in line with the rotating shaft and measured the rotating speed and torque produced by the rotating runner blade. A basin with a cylindrical shape was selected for the analysis. The centrifugal pump has the model number CP106B with a power rating of 1.5kW. A water flow meter with an open valve was connected to the pipe to measure the water flow rate. A diffuser with a 10-degree angle was used and installed at the inlet channel. A basin with a cylindrical shape was used in this analysis. A band brake is attached to a turbine shaft to control the rotation of the runner blade.

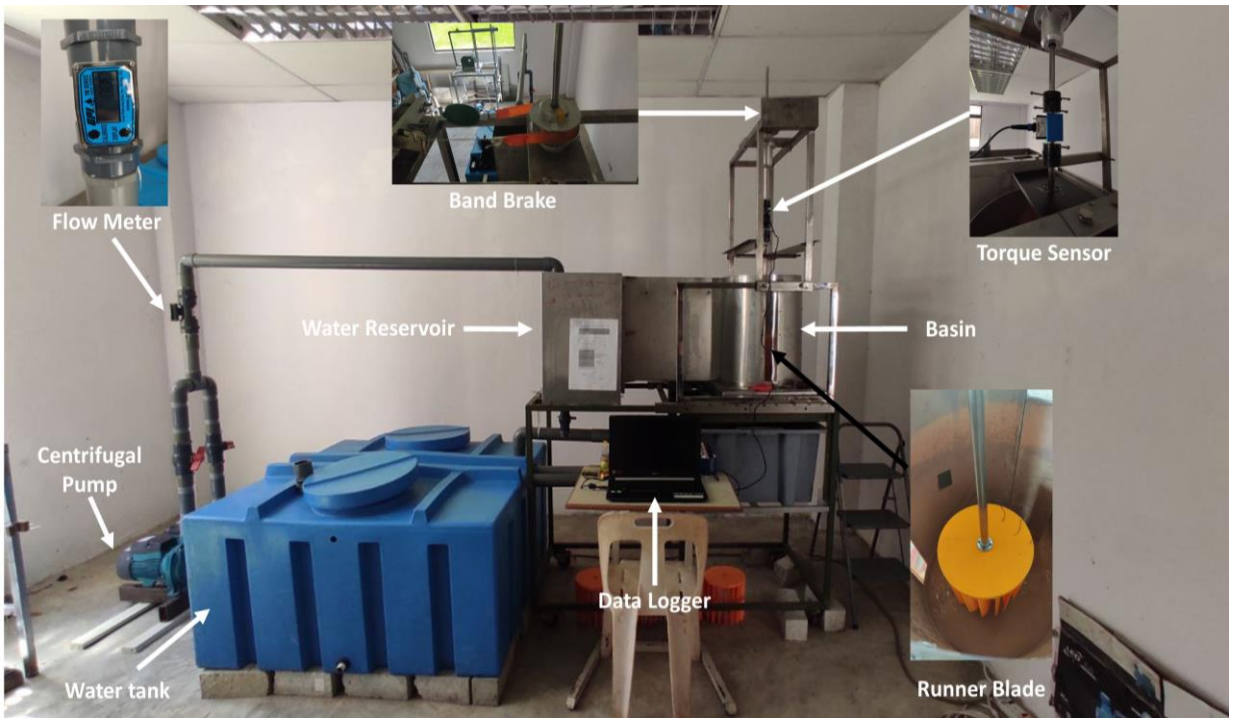

Fig. 7. Experimental setup

7. Specification of Crossflow Vortex Turbine

This turbine has a crossflow shape that has been adapted from Sritram and Suntivarakorn [12] previous studies. An overview of the crossflow vortex turbine is illustrated in Figure 8. The specifications are given in Table 2. The blade inlet diameter is D_i = 0.13m, the blade outlet diameter is D_o =0.20m, the blade thickness is t =0.015m, the height of the blade is b_1 =0.20m, the blade width is b_2 = 0.20m, and the number of blades is z =18.

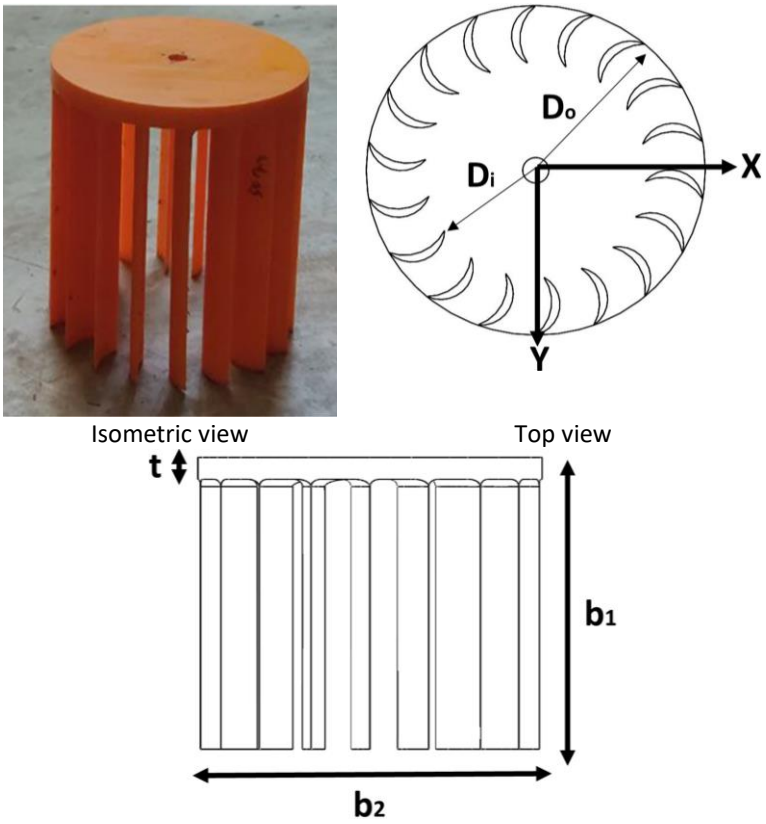

Fig. 8. Crossflow vortex turbine

Table 2
Specification of a crossflow vortex turbine

Parameter	Unit
Outer diameter, D_o	0.20 m
Inner diameter, D_{in}	0.13 m
Thickness, t	0.02 m
Height of the blade, b_1	0.02 m
Blade width, b_2	0.02 m
Number of blades, Z	18

Figure 9 shows the vector diagram as the reference blade geometry that has been used to identify the performance characteristic curves of the crossflow vortex turbine. This turbine was tested based on the same work conditions with the flow rate, head, water vortex height, and turbine position are 0.004 m^3/s, 0.23 m, 0.22 m, and 0.05 m respectively. The modified blade angles as a parameter variable for the design implementation of the crossflow vortex turbine are shown in Table 3. The four different blade angles were tested by controlling the rotational speed that have been measured using a torque sensor. Then, the torque, power output, and efficiency performance have been determined.

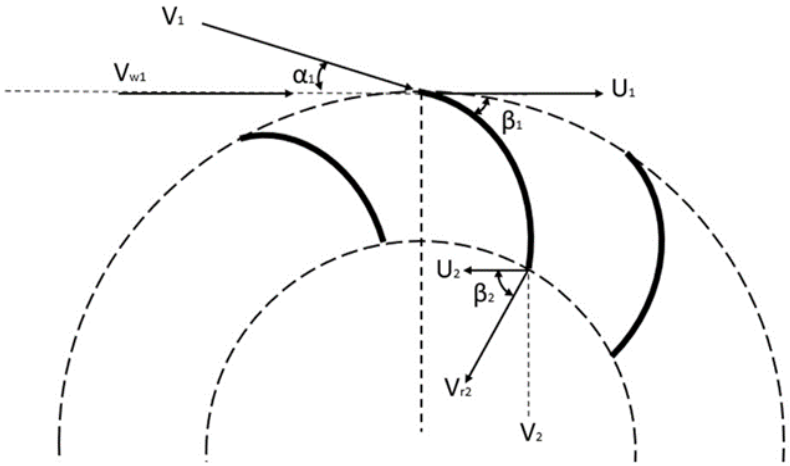

Fig. 9. The vector diagram of the Crossflow Blade

Table 3
Technical details for the design of crossflow vortex turbine

Type of turbine	Blade inlet angle, β_1 (°)	Blade outlet angle, β_2 (°)
Crossflow A	40	60
Crossflow B	50	55
Crossflow C	60	45
Crossflow D	70	40

The crossflow vortex turbine in the GWVPP system was allowed to run continuously for 5 minutes before readings from the sensor were recorded. This allowed the water to flow through a uniform water vortex in the basin and ensured that the sensors were recording consistent readings.

The rotational speed of the crossflow vortex turbine in the GWVPP system was adjusted to between 30 RPM and 70 RPM by adjusting the band brake that was applied to the rotating shaft. The turbine's corresponding torque, power output, and efficiency were measured and documented. The hydraulic power, mechanical power, and efficiency were determined based on the observed parameters and mathematical expression of energy conversion from Eq. (1), Eq. (3), and Eq. (4).

All measurements collected from the torque sensors were subjected to test setup limitations value of standard deviations from the data. It was presented to demonstrate how widely the measured values spread by the average data values [15]. The statistical analysis was provided to determine the experimental uncertainties by showing the accuracy and precision of the experimental results as shown in Figure 10 and Figure 11.

8. Performance Analysis of the Crossflow Vortex Turbine

The performance characteristics for crossflow vortex turbines A-D were presented as mechanical output parameters such as torque, power, and efficiency in Figure 10 to Figure 12. The performance curves are crucial to determine the optimum operation of turbomachinery [3]. In this case, the performance curves provide information on mechanical output parameters while indicating the best efficient point for rotational speed under constant flow rate and turbine position. As shown in Figure 10 to Figure 12, the crossflow turbine A-D produces power, torque, and efficiency with a similar trend at a rotational speed between 30-70 RPM. This demonstrates the inlet and outlet angle of the turbine produce mechanical power with different torque at tested rotational speed. The performance curves show torque, power, and efficiency at a given rotational speed that corresponds to the blade angle modification. Then, the crossflow vortex turbines A-D generate the highest power at the similar best

efficient point recorded at 50 RPM. At part load rotational speed, all crossflow vortex turbine (A-D) generates lower power with a parabolic trend. This is because the torque decreases with the increment of rotational speed, resulting in the lowest power among the crossflow vortex turbine (A-D) with approximately similar efficiency. The decreasing trend of the power with the increase in rotational speed is in parabolic behavior that shows an instantaneous reduction in the crossflow vortex turbine performance.

Figure 10 illustrates the performance curve of torque for four different blade angles at a rotational speed between 30-70 RPM. The highest torque generated by all the crossflow vortex turbines was found at the rotational speed of 30 RPM. This indicates higher torque was generated at a lower rotational speed and reduced to a lower value at a higher rotational speed. On the other hand, a higher torque was found at crossflow vortex turbine A, while the lower torque was at crossflow vortex turbine D. The increase in torque is attributed to the higher angular moment difference exerted by the inlet and outlet angle of the turbine blades. These results can be supported by the findings of Wichian and Suntivarakorn [16], who have reported that there is an increment in torque when the angular moment of the water flows increases.

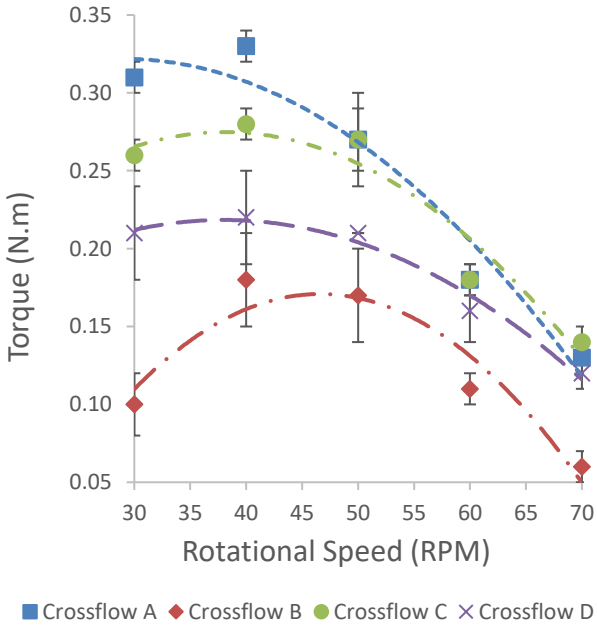

Fig. 10. Performance of crossflow turbine in terms of torque

Figure 11 shows the mechanical power outputs for four different blade angles. It can be found that the highest power is generated by all crossflow vortex turbines at 50 RPM. All turbines lose power when the rotational speed matches the tangential water vortex, which reduces the torque exerted on the turbine. Crossflow vortex turbine C has a maximum power output compared to other turbines, thereby indicating that the turbine has more energy extraction in the vortex. It was found the highest power output generated by the crossflow turbine C is 1.49±0.08 W at 50 RPM, generating the optimum torque at 0.27±0.02 N.m. Moreover, the relatively higher power generated by crossflow vortex turbine A than other turbines may be attributed to the large surface areas between the inlet and outlet angles of the blade. The possible reason for the slightly increased power in crossflow vortex turbine A also due to the high moment in the water catchment by the large normal area of the water flow direction [17].

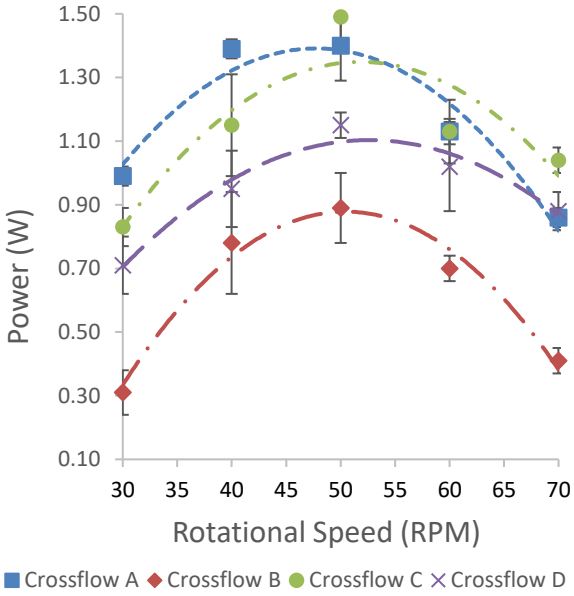

Fig. 11. Performance of crossflow turbine in terms of power

Figure 12 represents the turbine efficiency for four different blade angles that correspond to the rotational speed between 30-70 RPM. The efficiency for the crossflow vortex turbine is in line with the other researchers with reports in the range between 15-35%. The highest efficiency was polynomials at crossflow vortex turbine C. It was found that the efficiency of the crossflow vortex turbine C qualitatively follows the power generated. Other than that, crossflow vortex turbine C yields 18.98% maximum efficiency at a rotational speed of 50 RPM. Therefore, the best efficient point was found at 50 RPM as it has been identified to extract more power with optimum torque.

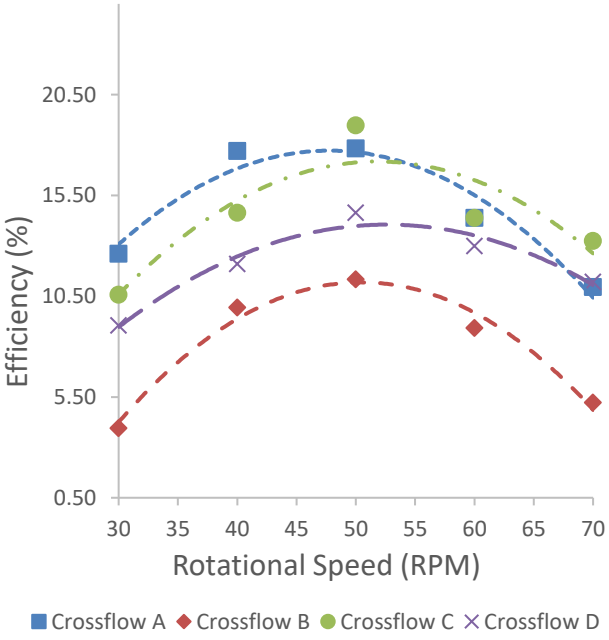

Fig. 12. Performance of crossflow turbine in terms of efficiency

9. Conclusions

A study on the feasibility of a gravitational water vortex power plant for the purpose of performance enhancement has been carried out with blade angle modification in the crossflow vortex turbine. The performance parameters of the turbine such as rotational speed, torque, power, and efficiency have been examined to determine the performance curves that are crucial in turbomachinery. In the crossflow vortex turbine, the performance parameters such as an inlet blade angle and outlet blade angle of 60^o and 45^o respectively are improved with the best operating speed of 50 RPM. The core findings of the present study are the following

i. The numerical study on the GWVPP asserted that the optimum hydraulic output such as water velocity profile and water tangential distribution can be obtained at the runner position of 0.05 m of the water vortex height.
ii. A significant reduction trend in the torque, power output, and efficiency was observed from the rotational speed at 60 RPM to 70 RPM in the crossflow vortex turbine.
iii. The performance curve of the crossflow vortex turbine is greatly affected by varying the angle of the blade. It is found that crossflow vortex turbine C provides maximum performance because of more water blade wetted area.
iv. Crossflow vortex turbine C shows a consistent performance with efficiency at 18.98% with the best operating speed of 50 RPM.

In summary, the blade profiles of the crossflow turbine crossflow must be designed in a manner that leads to minimal vortex distortion by maintaining the swirling vortex which can boost the performance of the gravitational water vortex turbine. The variation in efficiency performance strongly depends on the power output of turbine crossflow. Moreover, the increment in the rotational speed variation does not mainly increase the parameter's performance. The present study shows the rotational speed of 50 RPM as the best operating condition required to achieve the optimum performance of the turbine.

Acknowledgments

This work was supported by the Ministry of Higher Education Malaysia (MoHE) and Universiti Malaysia Sabah [GUG1072-2-2017]. This work was supported by the Ministry of Higher Education Malaysia (MoHE) [FRGS/1/2020/STG07/02/2] and Universiti Malaysia Sabah [GUG1072-2-2017].

Reference

[1] Huwae, Reza, Henny Sudibyo, Ridwan Arief Subekti, Anjar Susatyo, and Deni Shidqi Khaerudini. "A review: Gravitational water vortex power plant." In *2020 International Conference on Sustainable Energy Engineering and Application (ICSEEA)*, pp. 1-7. IEEE, 2020. https://doi.org/10.1109/ICSEEA50711.2020.9306140

[2] Sierra, Jorge, Alejandro Ruiz, Angie Guevara, and Alejandro Posada. "Review: Gravitational Vortex Turbines as a Renewable Energy." *International Journal of Fluid Machinery and Systems* 13, no. 4 (2020): 704-717. https://doi.org/10.5293/IJFMS.2020.13.4.704

[3] Ullah, Rizwan, Taqi Ahmad Cheema, Abdul Samad Saleem, Sarvat Mushtaq Ahmad, Javed Ahmad Chattha, and Cheol Woo Park. "Performance analysis of multi-stage gravitational water vortex turbine." *Energy Conversion and Management* 198 (2019): 111788. https://doi.org/10.1016/j.enconman.2019.111788

[4] Faraji, Adam, Yusufu Abeid Chande Jande, and Thomas Kivevele. "Performance analysis of a runner for gravitational water vortex power plant." *Energy Science & Engineering* 10, no. 4 (2022): 1055-1066. https://doi.org/10.1002/ese3.1085

[5] Dhakal, R., T. R. Bajracharya, S. R. Shakya, B. Kumal, K. Khanal, S. J. Williamson, S. Gautam, and D. P. Ghale. "Notice of Violation of IEEE Publication Principles: Computational and experimental investigation of runner for gravitational water vortex power plant." In *2017 IEEE 6Th International Conference on Renewable Energy Research and Applications (ICRERA)*, pp. 365-373. IEEE, 2017. https://doi.org/10.1109/ICRERA.2017.8191087

[6] Kayastha, Manil, Prashant Raut, Nirmal Kumar Subedi, Sandesh Tamang Ghising, and Rabin Dhakal. "CFD evaluation of performance of Gravitational Water Vortex Turbine at different runner positions." In *KEC Conference 2019*. 2019. https://doi.org/10.31224/osf.io/d9qn3

[7] Kueh, Tze Cheng, S. L. Beh, Y. S. Ooi, and D. G. Rilling. "Experimental study to the influences of rotational speed and blade shape on water vortex turbine performance." In *Journal of Physics: Conference Series*, vol. 822, no. 1, p. 012066. IOP Publishing, 2017. https://doi.org/10.1088/1742-6596/822/1/012066

[8] Nishi, Yasuyuki, Ryouta Suzuo, Daichi Sukemori, and Terumi Inagaki. "Loss analysis of gravitation vortex type water turbine and influence of flow rate on the turbine's performance." *Renewable Energy* 155 (2020): 1103-1117. https://doi.org/10.1016/j.renene.2020.03.186

[9] Aziz, Muhammad Qamaran Abdul, Juferi Idris, and Muhammad Firdaus Abdullah. "Experimental study on enclosed gravitational water vortex turbine (GWVT) producing optimum power output for energy production." *Journal of Advanced Research in Fluid Mechanics and Thermal Sciences* 95, no. 2 (2022): 146-158. https://doi.org/10.37934/arfmts.95.2.146158

[10] Del Rio, Jorge Andrés Sierra, Alejandro Ruiz Sánchez, Daniel Sanín Villa, and Edwin Correa Quintana. "Numerical Study of H-Darrieus Turbine as a Rotor for Gravitational Vortex Turbine." *CFD Letters* 14, no. 8 (2022): 1-11. https://doi.org/10.37934/cfdl.14.8.111

[11] Aziz, Muhammad Qamaran Abdul, Juferi Idris, and Muhammad Firdaus Abdullah. "Simulation of the conical gravitational water vortex turbine (GWVT) design in producing optimum force for energy production." *Journal of Advanced Research in Fluid Mechanics and Thermal Sciences* 89, no. 2 (2022): 99-113. https://doi.org/10.37934/arfmts.89.2.99113

[12] Sritram, Piyawat, and Ratchaphon Suntivarakorn. "The efficiency comparison of hydro turbines for micro power plant from free vortex." *Energies* 14, no. 23 (2021): 7961. https://doi.org/10.3390/en14237961

[13] Sánchez, Alejandro Ruiz, Jorge Andrés Sierra Del Rio, Angie Judith Guevara Muñoz, and José Alejandro Posada Montoya. "Numerical and experimental evaluation of concave and convex designs for gravitational water vortex turbine." *Journal of Advanced Research in Fluid Mechanics and Thermal Sciences* 64, no. 1 (2019): 160-172.

[14] Liu, Chengming, Tao Chen, Wenzhe Kang, Jianjun Kang, Lingjiu Zhou, Ran Tao, and Zhengwei Wang. "Study on Pressure Pulsation and Force Characteristics of Kaplan Turbine." *Water* 15, no. 13 (2023): 2421. https://doi.org/10.3390/w15132421

[15] Ismail, M. A., W. K. Muzammil, M. Rahman, M. W. K. Ibrahim, and S. Misran. "Experimental design and analysis of pump as turbine for microhydro system." In *IOP Conference Series: Materials Science and Engineering*, vol. 217, no. 1, p. 012014. IOP Publishing, 2017. https://doi.org/10.1088/1757-899X/217/1/012014

[16] Wichian, Pongsakorn, and Ratchaphon Suntivarakorn. "The effects of turbine baffle plates on the efficiency of water free vortex turbines." *Energy Procedia* 100 (2016): 198-202. https://doi.org/10.1016/j.egypro.2016.10.165

[17] Haryono, D. A., A. Fahruddin, A. Akbar, and M. Mulyadi. "The effect of blade angle on two-stage water turbine against power and efficiency." In *Journal of Physics: Conference Series*, vol. 1402, no. 4, p. 044044. IOP Publishing, 2019. https://doi.org/10.1088/1742-6596/1402/4/044044